A Dual-Electrode Approach for Highly Selective Detection of Glucose Based on Diffusion Layer Theory: Experiments and Simulation

Kang Wang, Dai Zhang, Ting Zhou, and Xing-Hua Xia*[a]

Abstract: A dual-electrode configuration for the highly selective detection of glucose in the diffusion layer of the substrate electrode is presented. In this approach, a glassy carbon electrode (GCE, substrate) modified with a conductive layer of glucose oxidase/Nafion/graphite (GNG) was used to create an interference-free region in its diffusion layer by electrochemical depletion of interfering electroactive species. A Pt microelectrode (tip, 5 μm in radius) was located in the diffusion layer of the GNG-modified GCE (GNG-G) with the help of scanning electrochemical microscopy. Consequently, the tip of the electrode could sense glucose selectively by detecting the amount of hydrogen peroxide (H_2O_2) formed from the oxidization of glucose on the glucose oxidase layer. The influences of parameters, including tip–substrate distance, substrate potential, and electrolyzing time, on the interference-removing efficiency of this dual-electrode approach have been investigated systematically. When the electrolyzing time was 30 s, the tip–substrate distance was $1.8a$ (9.0 μm) (where a is the radius of the tip electrode), the potentials of the tip and substrate electrodes were 0.7 V and 0.4 V, respectively, and a mixture of ascorbic acid (0.3 mM), uric acid (0.3 mM), and 4-acetaminophen (0.3 mM) had no influence on the glucose detection. In addition, the current–time responses of the tip electrode at different tip–substrate distances in a solution containing interfering species were numerically simulated. The results from the simulation are in good agreement with the experimental data. This research provides a concept of detection in the diffusion layer of a substrate electrode, as an interference-free region, for developing novel microelectrochemical devices.

Keywords: analytical methods · diffusion layer · glucose · scanning probe microscopy

Introduction

Improvement of the selectivity of biosensors remains an important aspect in the development of electrochemical detecting devices for biochemical analysis.[1–3] Glucose oxidase (GOD)-modified working electrodes are usually used for the purpose of specific response in the detection of glucose. Although the oxidation of glucose by GOD is highly specific, the detection principle of such a biosensor—usually the amperometric detection of the formed H_2O_2—is largely unspecific and, therefore, highly sensitive towards side reactions caused by chemical impurities. The main interferences come from the electrochemical oxidation of electroactive species, for example, ascorbic acid (AA), uric acid (UA) and 4-acetaminophen (4-AP). Traditional interference-removing methods include coating an additional selective or preoxidizing membrane on the front interface of the modified working electrode,[4–6] detecting glucose by means of a redox mediator, direct electron transfer between the enzyme and the electrodes,[7–12] and improving the electron-transfer turnover rate between the active site and the electrode.[11,12] Other interference-removing methods, such as enzyme microreactors,[13] bienzyme systems,[14] pre-electrolysis,[15] temperature variation,[16] and measuring cathodic current,[17,18] were also used to improve the selectivity of some electrochemical biosensors. For example, Prussian blue can electrocatalyze the reduction of H_2O_2 at a negative potential. At the reduction potential of H_2O_2, oxidation of interference species such as AA does not occur.[17–19]

Here, we report an alternative approach for depleting interfering electroactive species based on the theory of the electrochemical diffusion layer. When the electrochemical

[a] Dr. K. Wang, Dr. D. Zhang, T. Zhou, Prof. X.-H. Xia
The Key Laboratory of Life Analytical Chemistry
Department of Chemistry, Nanjing University
Nanjing 210093 (P. R. China)
Fax: (+86) 258-359-7436
E-mail: xhxia@nju.edu.cn

Supporting information for this article is available on the WWW under http://www.chemeurj.org/ or from the author. SEM image of the poly-PPD-GOD membrane and the electrochemical activity of the immobilized GOD in the above membrane.

 DOI: 10.1002/chem.200400587

oxidation of an interfering electroactive species is diffusion-controlled, its concentration on the electrode surface approaches zero and the concentration gradients in the diffusion layer are well defined by the Fick's laws. Therefore, an interference-free region is formed in the diffusion layer in close proximity to the electrode surface. In this case, when a probe electrode is positioned in the diffusion layer, the electrochemical signal for the interfering electroactive species should be negligible. Such an electrochemical depletion approach provides a reproducible and easily controllable method to improve the practical performance of biosensors and is promising for the fabrication of electrochemical microdevices, because of its capability to remove interference in the diffusion layer. Such a detection concept could open up a new way for the development of highly selective methods for glucose detection with two closely positioned working electrodes. In addition, quantitative investigation and theoretical simulations of electrochemical depletion would be helpful for designing interference-free electrochemical microdevices.

Scanning electrochemical microscopy (SECM) is a scanning probe microscopic technique that positions an ultramicroelectrode (UME, tip electrode) a few micrometers above a specimen to exploit faradic currents.[20–23] The tip current is a function of the tip–substrate distance and also depends on the nature of the substrate.[23] Therefore, an approach curve could be used to define the distance between the tip and the substrate. The detailed principle of the feedback mode of SECM has been described elsewhere.[24] Previous studies have proved that SECM was a powerful tool in biosensor research. The so-called feedback mode of SECM has been widely used in the research of microstructured, biochemically active surfaces. By scanning the tip laterally on the sample surface and simultaneously measuring the change of currents, the difference in reaction rates at different locations on the sample surface can be resolved.[25–33] An alternative way is to observe the enzymatic activity by using the generation–collection mode of SECM. In this detection mode the tip electrode acts as an amperometric probe and detects species generated from the substrate (e.g., H_2O_2 generated from the immobilized enzyme layer or patterns on the substrate surface).[34–38] Normally, enzymatic activity could be imaged on locally deposited enzyme patterns.[31,39–41]

We have co-immobilized GOD in an insulating matrix of poly-*p*-phenylenediamine and investigated its interference-removing ability in the diffusion layer using SECM.[24] In the present paper, we report on the construction of a catalytic biointerface that significantly promoted the electrooxidation of interfering electroactive species (ascorbic acid, uric acid, etc.). This results in very high selective detection of glucose on the one hand, and on the other hand, such a catalytic interface ensures the diffusion-controlled electrochemistry of these interfering electroactive species, which in turn makes it easier to simulate the interference-removing process. Therefore, the finite element method (FEM) was used to simulate this interference-removing process. As shown in Figure 1, a glassy carbon electrode (GCE) modified with a conductive layer of glucose oxidase/Nafion/graphite (GNG) was used as a substrate electrode to deplete interfering electroactive species. A Pt microelectrode was located in the diffusion layer of a GNG-modified GCE (GNG-G) by using SECM to sense the H_2O_2 generated from the oxidation of glucose on the GOD layer. The oxidation current of H_2O_2 at the tip electrode served as the response signal of glucose concentration. By independently applying a proper potential on the substrate electrode, electroactive species (e.g., AA) in the diffusion layer of the modified GCE could be depleted without consumption of H_2O_2. Thus, a relatively interference-free region was formed and highly selective glucose detection could be achieved on the tip electrode.

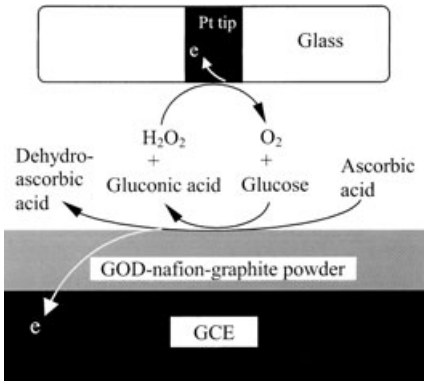

Figure 1. Scheme and principle of the approach for interference-removal in the diffusion layer of a GNG-G electrode.

Results and discussion

Characterization of the GNG layer: In this detection approach, a mixture of neutralized Nafion and graphite powder was used to form a conductive matrix layer that retains the bioactivity of the co-immobilized GOD. Neutralized Nafion was used for two reasons. Firstly, Nafion can conglutinate graphite powder easily and the resulting membranes possess a high adhesion to the electrode surface. Secondly, neutralized Nafion has been used to stabilize GOD through the formation of ammonium sulfate residues.[42] Scanning electron microscopy (SEM) characterization showed that the surface of the GNG layer was relatively smooth and the graphite pieces were uniformly dispersed (see Supporting Information, Figure S1). Therefore, localized detection of H_2O_2 generated on the GNG layer should reflect the situation on the whole of the GNG-G electrode surface.

The activity of the immobilized GOD was tested in a solution of glucose in a phosphate buffer solution (PBS; 20 mM, see Supporting Information, Figure S2). An anodic current of the enzyme-immobilized electrode in the glucose solution appeared at potentials higher than 0.45 V. This

anodic current results from the electrochemical oxidation of H_2O_2 generated in the enzymatic reaction of glucose with dissolved oxygen; this indicates that GOD in the matrix of Nafion/graphite has high activity. An approach curve of the Pt tip electrode to the GNG-G electrode was measured in an aqueous solution of KCl (0.1 M) containing $[Ru(NH_3)_6]Cl_3$ (1 mM). The tip current and the distance were normalized by $i_{T,\infty}$ and a, respectively, where $i_{T,\infty}$ is the steady-state tip current in bulk solution and a is the radius of the tip electrode. The obtained I_T versus L curve (Figure 2, open circles) shows a typical positive feedback, which fits well to the theoretically calculated one based on positive feedback for a pure conductor (Figure 2, solid curve). The observed pure positive feedback was then used to estimate the tip–substrate distance. In the present case, the calculated vertical position of the tip electrode is given relative to the top surface of the GNG layer.

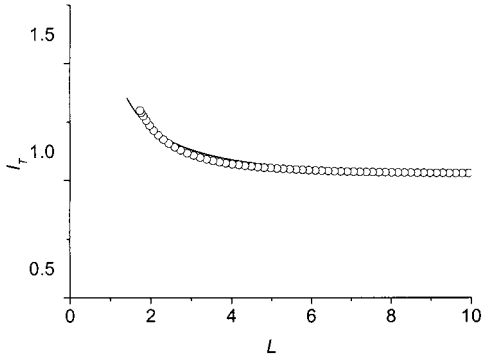

Figure 2. Normalized current–distance curves recorded with a Pt ultramicroelectrode (UME; $a = 5$ μm) in a phosphate buffer solution containing $[Ru(NH_3)_6]Cl_3$ (1 mM) (open circles). The solid curve denotes the theoretically calculated current–distance behavior for a conducting substrate.

Electrochemical properties of the glucose detection approach: Linear sweep votammograms of AA, UA, 4-AP, and H_2O_2 on the GNG-G and tip electrodes are shown in Figure 3. For the tip electrode (Figure 3b), the oxidation currents of the interfering electroactive species are relatively large, in spite of the electrocatalytic oxidation of H_2O_2 on platinum. In the case of the substrate electrode (Figure 3a), all these chemicals could be electrochemically oxidized on the GNG-G electrode in the applied potential window. The oxidation of the interfering electroactive species starts at more negative potentials (AA: < 0.0 V, UA and 4-AP: 0.2 V) relative to that for H_2O_2 oxidation (0.5 V). At potentials more positive than 0.3 V, the oxidation rates of the interfering electroactive species reach a diffusion-limited level. Therefore, by controlling the substrate electrode potential within the range of 0.3–0.4 V, the electroactive species in the diffusion layer of the GNG-G can be depleted. At the same time, H_2O_2 in the diffusion layer is not consumed, due to its higher oxidation overpotential. The diffusion layer of the GNG-G electrode thus creates an interference-free region for glucose detection by the tip electrode (as shown in Figure 1).

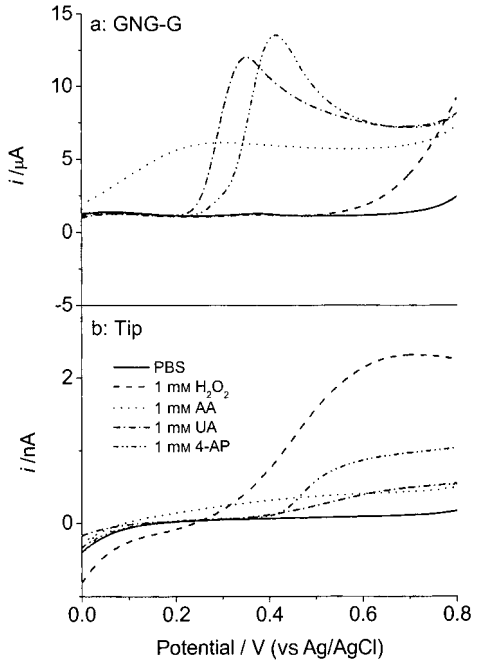

Figure 3. Linear sweep voltammograms of a GNG-G electrode (a) and a Pt tip electrode (b) in PBS (solid curve) and PBS containing H_2O_2 (1 mM; dashed curve), AA (1 mM; dotted curve), UA (1 mM; dash–dot curve), or 4-AP (1 mM; dash–dot–dot curve) at a scan rate of 5 mV s^{-1}.

In this glucose detection approach, the removal of interference is determined mainly by the electrochemical depletion of the interfering species on the substrate electrode and is not due to the electrostatic repulsion effect between Nafion and interfering species.[43] It should be noted that 1) Nafion used in our configuration was neutralized, so the negative charge of the membrane was negligible and 2) Nafion was mixed together with graphite powder and GOD instead of directly coating the outer side of the enzyme-modified electrode. Accordingly, interfering electroactive species were electrochemically depleted on the GNG-G electrode.

Parameters that influence the selectivity of glucose detection: The selectivity and sensitivity for the detection of glucose by the tip electrode in the diffusion layer of the GNG-G electrode depends on the tip–substrate distance, owing to the existence of a concentration gradient of both the electroactive species and the generated H_2O_2 in the tip–substrate gap. Figure 4 shows the influence of the tip–substrate distance on the detection of glucose and the removal of AA. In these measurements, a substrate potential of 0.4 V was used. With regards to the measurements performed on a solution of AA, the difference between the tip currents with ($i_{T,AA}$) and without AA ($i_{T,PBS}$) drops almost linearly with the decrease of the normalized tip–substrate distance L ($L = d/a$ where d is the tip–substrate distance). When the normalized tip–substrate distance was less than 4, no difference in the

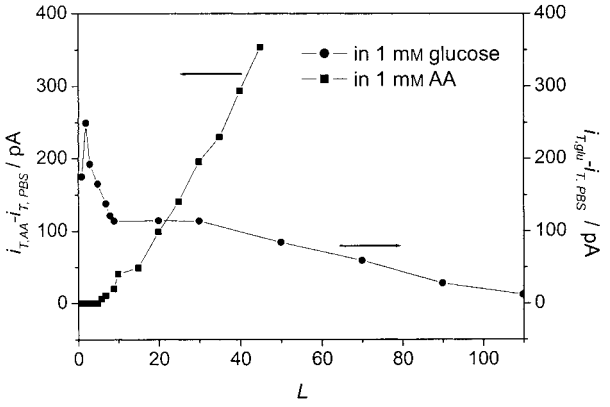

Figure 4. Dependence of the tip current difference ($i_{T,AA}-i_{T,PBS}$) and ($i_{T,glu}-i_{T,PBS}$) on the normalized tip–substrate distance. Filled squares: in 1 mM AA; filled circles: in 1 mM glucose. Tip potential: 0.7 V, substrate potential: 0.4 V.

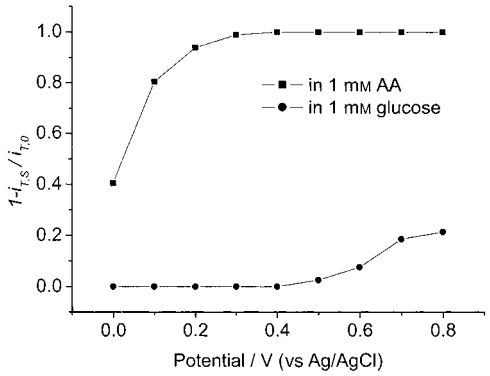

Figure 5. Dependence of the interference-removing efficiency on the substrate potential. The tip–substrate distance was kept at 1.8a (9.0 μm) and the tip currents were taken at the polarization time of 30 s. The corresponding $i_{T,0}$ of the tip electrode was taken with the substrate electrode at open-circuit. $E_T=0.7$ V.

two currents was observed, demonstrating that AA could be completely depleted by the substrate electrode. In contrast, in the solution of glucose (1 mM), the tip current difference (with glucose: $i_{T,glu}$; without glucose: $i_{T,PBS}$) increases gradually with decreasing tip–substrate distance. Within a smaller tip–substrate distance ($L<9$), the tip current difference increases rapidly with decreasing tip–substrate distance. This increase can be attributed to the increase of H_2O_2 concentration near the GNG-G electrode. At the normalized distance of 1.8, the tip current reaches a peak value, and then decreases further as the tip approaches the substrate ($L=0.8$). This decrease is caused by the sealing glass of the tip electrode, which hinders the diffusion of glucose from the bulk solution to the tip–substrate gap and in turn blocks the formation of H_2O_2. Therefore, measurements at a normalized tip–substrate distance of 1.8 (corresponding to 9.0 μm) can give results with high sensitivity for the detection of glucose. At this fixed distance, the sensor shows a good reproducibility (RSD = 2.2%, $n=5$, where RSD is the relative standard deviation and n is the number of tested samples).

The tip currents with ($i_{T,S}$) or without ($i_{T,0}$) applying a substrate potential were measured to evaluate the influence of the substrate potential on the interference-removing efficiency. Here, the interference-removing efficiency measured in a solution of AA is defined as $1-i_{T,S}/i_{T,0}$. On the other hand, when measurements were performed in the presence of glucose, this value represents the percentage of H_2O_2 in the tip–substrate gap that was consumed by the substrate electrode. Figure 5 shows the relationship between the substrate potential and the value of $1-i_{T,S}/i_{T,0}$. In these experiments, the normalized tip–substrate distance was kept at 1.8a, and the tip currents (at a tip potential of 0.7 V) were taken at a polarization time of 30 s. In a solution containing AA (1 mM, filled squares), the interference-removing efficiency increased with the increase of substrate potential, indicating that better interference-removing capability could be achieved with more positive substrate potentials. When the substrate potential was higher than 0.4 V, the interference-removing efficiency reached 100%. For measurements in a solution containing glucose (1 mM, filled circles) and with the substrate potential higher than 0.4 V, the value of $1-i_{T,S}/i_{T,0}$ increased gradually, due to the oxidation of the generated H_2O_2 at the GNG-G electrode. Therefore, 0.4 V is a proper substrate potential for effectively eliminating AA by means of a diffusion-limited reaction without consuming H_2O_2.

Glucose detection in a solution containing interference species: Figure 6 displays the time-dependent amperometric dynamic responses of the tip electrode ($E_T=0.7$ V). In the cases of solutions that did not contain electroactive species, with (curves a and c) or without (curves b and d) a potential

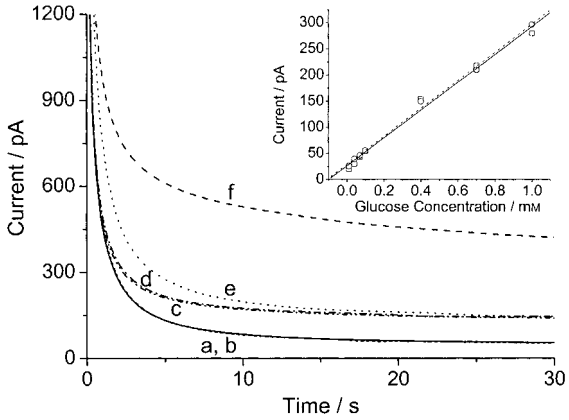

Figure 6. Amperometric dynamic responses of a Pt tip electrode with and without applying a potential of 0.4 V to the substrate electrode. The tip–substrate distance was kept at 1.8a (9.0 μm). a), b): PBS; c), d): glucose (1 mM); e), f): AA (0.3 mM), UA (0.3 mM), 4-AP (0.3 mM), and glucose (1 mM). Curves a), c), and e) were recorded with applying a potential of 0.4 V on the substrate electrode; curves b), d), and f) were recorded with the substrate electrode at open circuit. $E_T=0.7$ V. Inset: dependence of the tip currents on the concentration of glucose. Dashed line corresponds to the open circles: glucose solutions with AA (0.3 mM), UA (0.3 mM), and 4-AP (0.3 mM); solid line corresponding to the open squares: pure glucose solutions.

applied to the substrate electrode, the tip currents overlap well, demonstrating that the applied substrate potential does not affect the tip current in the solutions of PBS or glucose. For the mixture containing glucose, AA, UA, and 4-AP, when no external potential was applied on the substrate electrode, the obtained steady-state tip current (curve f) was much higher than those obtained in curves c and d, indicating that the electroactive species strongly interfere with the glucose detection. However, when applying a potential of 0.4 V on the substrate electrode (curve e), the tip current dropped dramatically, leading to the same response (curve e) as that depicted in curves c and d (without electroactive species) after the polarization time of 25 s. The decrease of the tip current confirms that the substrate electrode selectively consumed the interfering electroactive species at the applied potential.

Calibration curves were obtained for different concentrations of glucose with (Figure 6 inset, dashed line corresponds to open circles) or without AA, UA, and 4-AP (Figure 6 inset, solid line corresponds to open squares). These two calibration lines lead to almost the same results in the tested glucose concentrations. The linear range of glucose detection is 1.0×10^{-5}–1.0×10^{-3} M with a correlation coefficient of 0.9979 (with interfering electroactive species).

Numerical simulation of the interference-removal process: As shown in Figure 3, the kinetics of the electrooxidation of interfering species (AA, UA, and 4-AP) on GNG-G (at 0.4 V) and tip electrodes (at 0.7 V) is diffusion-controlled. When a potential of 0.4 V is applied to the substrate, the interfering species at the substrate surface is depleted immediately and a time-dependent concentration gradient appears along the direction perpendicular to the substrate surface. Meanwhile, diffusion of the interfering species from outside solution (bulk) to the tip–substrate gap will inevitably be inhibited, due to the large surface area of the sealing glass wall. Taking the above two factors into account, we used the finite element method (FEM) to simulate the interference-removal process. By using cylindrical coordinates, the time-dependent diffusion problems for interfering species can be written in dimensionless form as Equation (1)[44] (see Figure 7), in which L is the normalized tip-substrate distance ($L=d/a$).

$$\frac{\partial C_i}{\partial \tau}=\frac{\partial^2 C_i}{\partial z^2}+\frac{\partial^2 C_i}{\partial R^2}+\frac{1}{R}\frac{\partial C_i}{\partial R}\quad 0<\tau,0\le R,0<Z<L \tag{1}$$

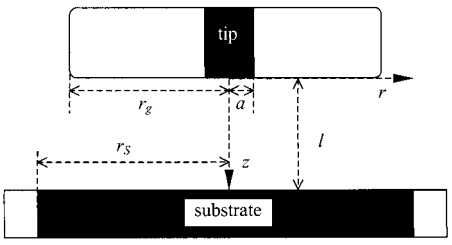

Figure 7. Schematic representation of the simulation domain and the parameters defining the diffusion problem for SECM.

The dimensionless variables are defined by $R=r/a$, $Z=z/a$, $C_i=c_i/C_i^o$, $\tau=tD/a^2$, in which r and z are the coordinates in the directions radial and normal to the electrode surface, respectively; D and c_i are the diffusion coefficient and concentration of interfering species; C_i^o is the bulk concentration of interfering species; a is the tip electrode radius; and t is time. Because the electrooxidation of the interfering electroactive species (e.g., ascorbic acid) is an irreversible process, the boundary conditions for the problem under these conditions are: 1) when $\tau=0$: $C_i=1$; 2) when $0<\tau$: $0\le R<1$ $Z=0$ (tip electrode surface), $C_i=0$, $\partial C_i/\partial Z=J_T$ (in which J_T is the normalized flux of interfering species at the tip electrode); $1\le R\le RG$ $Z=0$ ($RG=r_g/a$, glass insulating sheath), $\partial C_0/\partial Z=0$; $0\le R\le h$ $Z=L$ ($h=r_s/a$, $L=L/a$, substrate electrode surface), $C_i=0$ (when a diffusion-controlled oxidizing potential is applied on the substrate electrode), $\partial C_i/\partial Z=0$ (when no potential is applied on the substrate electrode). The solution of this problem can be obtained in terms of the dimensionless current I_T [Eq. (2)].

$$I_T(\tau)=-\frac{\pi}{2}\int_0^1 J_T(\tau,R)R\,dR \tag{2}$$

Figure 8 shows the simulated tip currents at different tip–substrate distances. In Figure 8a, only the tip electrode is polarized at a diffusion-controlled potential. In Figure 8b, both the tip and substrate electrodes are polarized at diffusion-controlled potentials. When there is no potential applied to

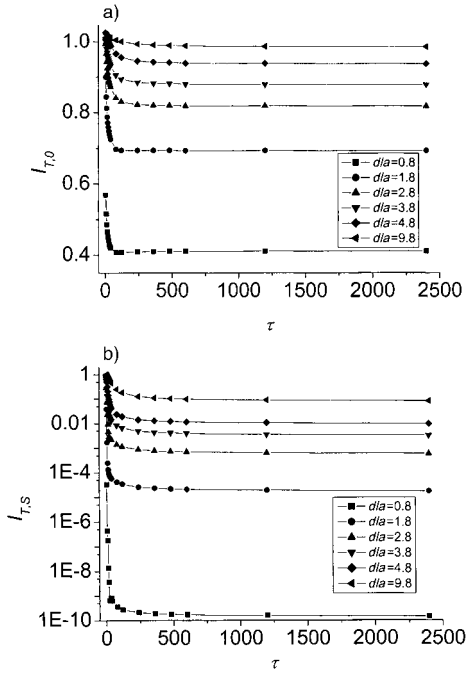

Figure 8. Simulated tip currents in a solution containing interfering electroactive species at different tip–substrate distances. a) A diffusion-controlled potential applied on only the tip electrode, while the substrate electrode is at open circuit; b) diffusion controlled potentials applied on both the tip and substrate electrodes.

the substrate electrode (Figure 8a), the normalized tip currents at different tip–substrate distances decrease dramatically at the beginning, and then reach a relatively constant value (typically, $\tau > 80$). However, with the application of a positive potential (i.e., 0.4 V) to the substrate electrode, the normalized tip current drops abruptly when $\tau > 20$, and then reaches a constant value (typically, $\tau > 40$). In both cases, the tip currents are prone to decrease at the closer tip–substrate distances. However, the tip current decreases much more rapidly when the electrochemical depletion of interfering species is functioning. Table 1 shows the ratio of $I_{T,S}$ to $I_{T,O}$ at different tip–substrate distances. With the shorter tip–substrate distance, this ratio decreases rapidly, indicating that a shorter tip–substrate distance can give a higher interference-removing efficiency. This result is consistent with that shown in Figure 4. At the same time, the tip current ratios decrease with the increase of normalized time τ, that is, between $\tau = 40$ and $\tau = 480$ the ratio decreases from 1/418 to 1/1340 at a normalized tip–substrate distance of 2.8. This result demonstrates that the interference-removing efficiency increases with the increase of the polarization time. These results are reasonably consistent with those obtained in our practical system, as shown in Figure 6. Evidently, the present approach has high interference-removing efficiency.

Table 1. Ratio of the simulated tip currents ($I_{T,S}/I_{T,0}$) at different tip-substrate distances.

	$I_{T,S}/I_{T,0}$					
Normalized	Normalized tip–substrate distance d/a					
time τ	0.8	1.8	2.8	3.8	4.8	9.8
40	1.40×10^{-9}	7.56×10^{-5}	0.0024	0.013	0.040	0.43
80	8.42×10^{-10}	5.58×10^{-5}	0.0016	0.0087	0.023	0.23
120	6.29×10^{-10}	4.66×10^{-5}	0.0013	0.0070	0.019	0.17
240	4.76×10^{-10}	3.43×10^{-5}	9.76×10^{-4}	0.0045	0.014	0.12
480	3.78×10^{-10}	2.77×10^{-5}	7.89×10^{-4}	0.0041	0.011	0.092

Conclusion

A novel approach with high selectivity for the detection of glucose has been established based on the electrochemical depletion of interfering electroactive species in the diffusion layer of a substrate electrode. Factors influencing the selectivity of glucose detection were systematically investigated by using SECM. Both the experimental and simulation results showed that this interference-removing approach is a promising scheme for constructing electrochemical microdevices. Furthermore, the tip and the substrate electrode can be printed on a chip at an optimal distance, which makes this configuration promising for practical applications.

Experimental Section

Chemicals: Glucose oxidase (EC 1.1.3.4, 200,000 U g^{-1}, Sigma) was used as received. Nafion (wt. 5% solution) and graphite powder (1–2 μm in diameter) were from Aldrich. $[Ru(NH_3)_6]Cl_3$ (Aldrich), uric acid (Lancaster), ascorbic acid, glucose, and phosphate (Nanjing, China) were of analytical grade. 4-Acetaminophen (Nanjing, China) was of reagent grade. Glucose was dissolved in 0.05 M phosphate buffer solution (PBS, pH 7.4, containing 0.1 M KCl). All solutions were prepared with 18.2 MΩ deionized water (Purelab Classic Corp., USA).

SECM system: A model CHI 900 SECM (CH Instruments, USA) was used for the measurement of approach curves. The SECM tip was a Pt microelectrode ($a = 5$ μm, isolating glass outer wall radius r_g : $a = 10$). All electrochemical measurements were performed in a Teflon cell (ca. 2 mL). A four-electrode system was used for all measurements with a Pt wire as counter electrode, Ag/AgCl (in 3 M KCl) as reference electrode, and the Pt tip as the first working electrode. A glassy carbon disk electrode (GCE, 3.5 mm in diameter) modified with a GOD-Nafion-graphite powder layer was used both as the second working electrode and the substrate of SECM. Before each measurement, the Pt microelectrode was polished with 0.05 μm alumina slurry on microcloth pads. Prior to glucose detection, the SECM tip electrode was firstly positioned above the sample surface by approaching the sample surface in 1 mM $[Ru(NH_3)_6]Cl_3$ (1 mM) with a tip potential of −0.3 V. At this potential, $[Ru(NH_3)_6]Cl_3$ was reduced according to the reaction given in Equation (3).

$$[Ru(NH_3)_6]^{3+} + e^- \rightarrow [Ru(NH_3)_6]^{2+} \quad (3)$$

The tip was stopped when the tip current reached 125% of the steady-state diffusion-controlled tip current in bulk solution ($i_{T,\infty}$). The tip–substrate distance was then determined by comparing the measured cathodic current with the normalized current–distance (I_T–L).[6] Sample solutions were then added into the cell after rinsing with PBS (×4; ca. 20 s for each time) to remove any $[Ru(NH_3)_6]Cl_3$ remaining in the tip–substrate gap. A steady potential was applied on the tip electrode and the current–time curves were recorded.

Fabrication of GOD-modified substrate electrode: We improved the immobilization process of GOD reported by Karyakin and co-workers.[42] In our case, the glassy carbon electrode was polished with alumina (0.05 μm) and sonicated in water before modification. Nafion solution (300 μL, wt. 5%) was neutralized by an aqueous solution of ammonia (5 μL, wt. 25%) up to pH 5.5. The neutralized Nafion solution was diluted to 1% by adding absolute ethanol (1195 μL). This Nafion solution (100 μL, 1%) was then added into 10 mg graphite powder and mixed under ultrasound for 30 min. A solution of GOD (10 μL; 100 mg mL^{-1}, in PBS pH 7.4) was introduced to the resultant mixture. After thoroughly stirring, 5 μL of the final mixture was dropped onto the cleaned glassy carbon electrode and the solvent was allowed to evaporate at a temperature of 4 °C for 30 min. Finally, the formed GNG-G electrode was dipped in PBS (pH 7.4) for 5 min and was stored at 4 °C before use.

Acknowledgement

This work was supported by grants from the National Natural Science Foundation of China (NSFC, No. 20125515; 20299030; 20375016).

[1] T. Inoue, J. R. Kirchhoff, R. A. Hudson, *Anal. Chem.* **2002**, *74*, 5321–5326.
[2] X. H. Yang, S. B. Hall, S. N. Tan, *Electroanalysis* **2003**, *15*, 885–891.
[3] T. M. H. Lee, L. L. Li, I. M. Hsing, *Langmuir* **2003**, *19*, 4338–4343.
[4] L. Ying, E. T. Kang, K. G. Neoh, *J. Membr. Sci.* **2002**, 208, 361–374.
[5] S. Myler, S. D. Collyer, K. A. Bridge, S. P. J. Higson, *Biosens. Bioelectron.* **2002**, *17*, 35–43.
[6] J. H. Yu, H. X. Ju, *Anal. Chem.* **2002**, *74*, 3579–3583.

[7] T. Z. Peng, Q. Chen, R. C. Stevens, *Anal. Chem.* **2000**, *72*, 1611–1617.
[8] X. Chen, S. J. Dong, *Biosens. Bioelectron.* **2003**, *18*, 999–1004.
[9] J. J. Gooding, R. Wibowo, J. Q. Liu, W. R. Yang, D. Losic, S. Orbons, F. J. Mearns, J. G. Shapter, D. B. Hibbert, *J. Am. Chem. Soc.* **2003**, *125*, 9006–9007.
[10] K. F. Aguey-Zinsou, P. V. Bernhardt, U. Kappler, A. G. McEwan, *J. Am. Chem. Soc.* **2003**, *125*, 530–535.
[11] Y. Xiao, F. Patolsky, E. Katz, J. F. Hainfeld, I. Willner, *Science* **2003**, *299*, 1877–1881.
[12] I. Willner, V. H. Shabtai, R. Blonder, E. Katz, G. L. Tao, A. F. Buckmann, A. Heller, *J. Am. Chem. Soc.* **1996**, *118*, 10321–10322.
[13] A. Collins, E. Mikeladze, M. Bengtsson, M. Kokaia, T. Laurell, E. Csoregi, *Electroanalysis* **2001**, 13, 425–431.
[14] L. Q. Mao, P. G. Osborne, K. Yamamoto, T. Kato, *Anal. Chem.* **2002**, *74*, 3684–3689.
[15] C. E. Lunte, T. H. Ridgway, W. R. Heineman, *Anal. Chem.* **1987**, *59*, 761–766.
[16] C. Lau, S. Reiter, W. Schuhmann, P. Grundler, *Anal. Bioanal. Chem.* **2004**, 379, 255–260.
[17] A. A. Karyakin, E. E. Karyakina, L. Gorton, *Anal. Chem.* **2000**, *72*, 1720–1723.
[18] A. A. Karyakin, E. E. Karyakina, L. Gorton. *Electrochem. Commun.* **1999**, *1*, 78–82.
[19] D. Zhang, K. Zhang, Y. L. Yao, X. H. Xia, H. Y. Chen, *Langmuir* **2004**, *20*, 7303–7307.
[20] J. Kwak, A. J. Bard, *Anal. Chem.* **1989**, *61*, 1794–1799.
[21] A. J. Bard, F. R. F. Fan, J. Kwak, O. Lev, *Anal. Chem.* **1989**, *61*, 132–138.
[22] R. D. Martin, P. R. Unwin, *Anal. Chem.* **1998**, *70*, 276–284.
[23] J. Kwak, A. J. Bard, *Anal. Chem.* **1989**, *61*, 1221–1227.
[24] K. Wang, J. J. Xu, D. C. Sun, H. Wei, X. H. Xia, *Biosens. Bioelectron.* **2004**, *20*, 1366–1372.
[25] S. Kasai, A. Yokota, H. F. Zhou, M. Nishizawa, K. Niwa, T. Onouchi, T. Matsue, *Anal. Chem.* **2000**, *72*, 5761–5765.
[26] J. M. Liebetrau, H. M. Miller, J. E. Baur, *Anal. Chem.* **2003**, *75*, 563–571.
[27] J. Wang, F. M. Zhou, *J. Electroanal. Chem.* **2002**, *537*, 95–102.
[28] J. F. Zhou, C. Campbell, A. Heller, A. J. Bard, *Anal. Chem.* **2002**, *74*, 4007–4010.
[29] S. Kasai, Y. Hirano, N. Motochi, H. Shiku, M. Nishizawa, T. Matsue, *Anal. Chim. Acta* **2002**, *458*, 263–270.
[30] S. Gaspar, M. Mosbach, L. Wallman, T. Laurell, E. Csoregi, W. Schuhmann, *Anal. Chem.* **2001**, *73*, 4254–4261.
[31] I. Turyan, T. Matsue, D. Mandler, *Anal. Chem.* **2000**, *72*, 3431–3435.
[32] D. T. Pierce, P. R. Unwin, A. J. Bard, *Anal. Chem.* **1992**, *64*, 1795–1804.
[33] G. Wittstock, R. Hesse, W. Schuhmann, *Electroanalysis* **1997**, *9*, 746–750.
[34] C. A. Wijayawardhana, G. Wittstock, H. B. Halsall, W. R. Heineman, *Anal. Chem.* **2000**, *72*, 333–338.
[35] C. Zhao, J. K. Sinha, C. A. Wijayawardhana, G. Wittstock, *J. Electroanal. Chem.* **2004**, *561*, 83–91.
[36] C. A. Wijayawardhana, G. Wittstock, H. B. Halsall, W. R. Heineman, *Electroanalysis* **2000**, *12*, 640–644.
[37] G. Wittstock, K. J. Yu, H. B. Halsall, T. H. Ridgway, W. R. Heineman, *Anal. Chem.* **1995**, *67*, 3578–3582.
[38] B. R. Horrocks, D. Schmidtke, A. Heller, A. J. Bard, *Anal. Chem.* **1993**, *65*, 3605–3614.
[39] C. A. Zhao, G. Wittstock, *Anal. Chem.* **2004**, *76*, 3145–3154.
[40] T. Wilhelm, G. Wittstock, *Electrochim. Acta* **2001**, *47*, 275–281.
[41] G. Wittstock, W. Schuhmann, *Anal. Chem.* **1997**, *69*, 5059–5066.
[42] A. A. Karyakin, E. A. Kotel'nikova, L. V. Lukachova, E. E. Karyakina, J. Wang, *Anal. Chem.* **2002**, *74*, 1597–1603.
[43] D. R. Shankaran, N. Uehara, T. Kato, *Biosens. Bioelectron.* **2003**, *18*, 721–728.
[44] A. J. Bard, M. V. Mirkin, P. R. Unwin, D. O. Wipf, *J. Phys Chem.* **1992**, *96*, 1861–1868.

Received: June 10, 2004
Revised: September 9, 2004
Published online: January 10, 2005

